Time-Resolved Multispectral Imaging Spectrometer

OLEG KHAIT, SERGEV SMIRNOV, and CHIEU D. TRAN*

Department of Chemistry, Marquette University, P.O. Box 1881, Milwaukee, Wisconsin 53201

A new multispectral imaging spectrometer with millisecond resolution has been developed. This instrument is based on the use of an acousto-optic tunable filter (AOTF) for spectral tuning and a simple progressive scan camera capable of snapshot operation for recording. The fast multispectral imaging can be performed in two configurations: recording images as a function of time or as a function of wavelength. In the first configuration, multiple images are recorded, grabbed, and stored per one wavelength. Upon completion, the AOTF is scanned to a new recording wavelength and a new set of images are recorded. It was found that, in this configuration, the imaging spectrometer is capable of recording, grabbing, and storing up to 33 images per s (i.e., 30 ms per image). Because an external signal is used to start the event and the recording of images, and the period between the start of the event and the recording and grabbing of images can be appropriately adjusted by a delay line, the time resolution of the spectrometer is not limited to 30 ms but rather can be adjusted to a shorter or longer time scale. In the second configuration, the recording wavelength is rapidly scanned (by the AOTF) and only one image is rapidly recorded, grabbed, and stored for each wavelength. Because additional time is needed to scan the AOTF, the maximum number of images that can be grabbed in this case is 16 frames per s. Preliminary applications of the imaging spectrometer include measurements of photoinduced changes in temperature-sensitive cholesteric liquid crystals as a function of time and wavelength. It was found that irradiating with a near-infrared (NIR) diode laser of 805 nm led to changes in the liquid crystal. The changes were found to vary with time and wavelength, namely, at about 360 ms after the NIR laser pulse the liquid crystal underwent changes in the visible region around 570 nm. The changes shifted toward longer wavelength concomitantly with time; i.e., maximum change at about 600 ms shifted to 718 nm.

Index Headings: **Acousto-optic tunable filter; Multispectral imaging; Liquid crystal.**

INTRODUCTION

Multispectral imaging is a technique that can simultaneously record spectral and spatial information of a sample, i.e., the recorded images contain signals that are generated by a sample, and plotted as a function of spectral and spatial distribution[1]. Recent available fast scanning electronic tunable filters [acousto-optic tunable filters (AOFTs)[2,3] and liquid crystal tunable filters (LCTFs)[4]], Fourier transform interferometers[5,6] and area cameras [silicon, InGaAs, InSb, and HgCdTe, and the quantum well infrared photodetector (QWIP)] have made it possible for many research groups to develop novel multispectral imaging instruments that can rapidly and sensitively record spectral images in the UV, visible, near- and middle-infrared region.[4–13] Studies that to date were not possible can now be performed by using these newly developed instruments. These include the determination of the chemical inhomogeneity of polymers,[7,8,14] the authentication of stock certificate and currency,[7] the evidence of kinetic inhomogeneity,[8] and the detection of solid-phase peptide synthesis mediated by a solid-phase combinatorial chemical method.[9] It should be added that, in addition to the multispectral imaging technique, there are other techniques including those based on fiber-optic bundles[15] and line illumination[16] that can also provide images of a sample. However, in contrast to the multispectral imaging technique, elaborate data treatment may be needed to extract images from data recorded by these techniques.

It is of particular importance to increase the speed of the multispectral imaging instrument. Faster speeds will make it possible to study samples that undergo fast chemical, biochemical, or photochemical reactions. For samples that do not undergo chemical transformation during the measurement time, it would increase the signal-to-noise (S/N) of the measurement because multiple images can be rapidly recorded for subsequent signal averaging. Many factors that govern the speed of images are captured in the multispectral imaging technique. These include the speed of the tunable filter, the camera, and the frame grabber. The LCTF[4] and the AOTF[2,3] are two of the fastest electronic tunable filters currently available. Of the two, the AOTF is relatively faster than the LCTF because the tuning speed of the former is based on the speed of sound in a crystal, which is on the order of microseconds, whereas the latter is based on the response of the liquid crystal, which is on the order of milliseconds.[2–4]

In addition to the rapid recording of images, it is essential that a camera can be externally controlled (i.e., triggered) so that recorded images can be synchronized with events occurring in a sample. Such requirements can be satisfied with cameras that have become commercially available recently. In addition to the high sensitivity and the rapid recording of images, these high-performance cameras can operate in the ''snapshot'' mode in which an external signal can be used to trigger the recording of individual images.

The information presented is indeed provocative and clearly indicates that it is possible to use the AOTF and a high-performance camera to develop a novel multispectral imaging instrument that can rapidly record images of a sample. The instrumentation development of the multispectral imaging spectrometer and its utilization to study changes in a liquid crystal induced by irradiation with a near-infrared (NIR) pulsed laser will be demonstrated in this paper.

EXPERIMENTAL

Time-resolved multispectral micro-imaging of a sample was performed with the instrument shown in Fig. 1. As illustrated, a single-mode 805 nm diode laser powered by an ILX Lightwave power supply (Model LDX 3565) was used as the heating source for the sample. The laser can be operated in either continuous or pulse mode with

Received 26 June 2000; accepted 27 August 2000.

* Author to whom correspondence should be sent.

0003-7028/00/5412-1734$2.00/0

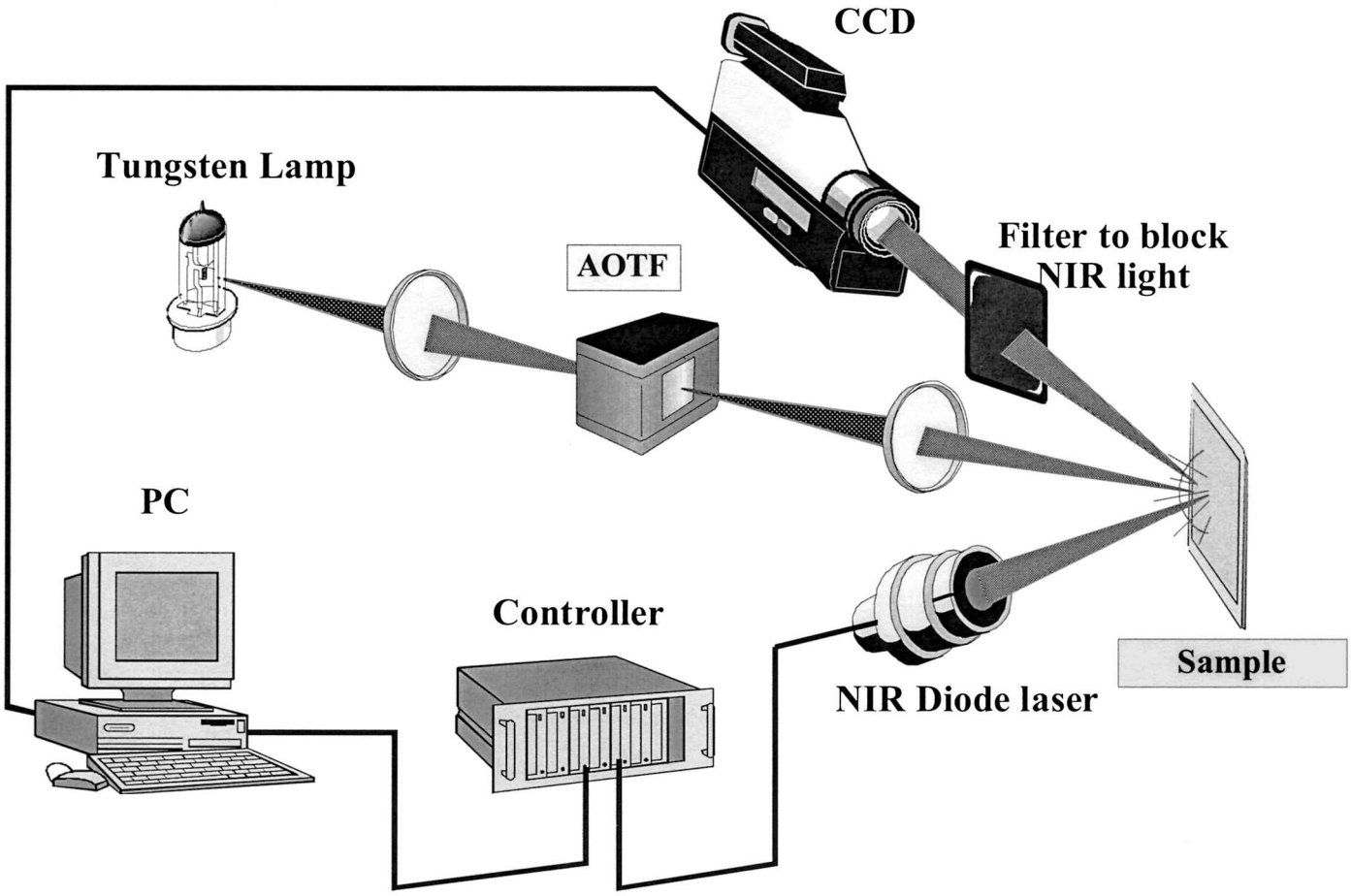

FIG. 1. Schematic diagram of the time-resolved multispectral imaging spectrometer.

adjustable pulse lengths. Changes in the sample induced by the NIR pulsed diode laser irradiation were measured by use of a 250 W halogen tungsten lamp as the light source. Prior to being incident to the sample, the output of this lamp was spectrally tuned by a noncolinear AOTF fabricated from TeO_2 (Matsushita Electronics Model EFL-F20R2). The AOTF was driven by a home-built radio-frequency (rf) driver, which is the same as that used in our earlier studies.[17,18] Light reflected from the sample was detected by an 8-bit 512 × 512 (10 μm × 10 μm pixel size) progressive scan silicon area camera (Dalsa Corporation Model CA-D8). This camera was operated in the snapshot mode; namely, the recording of images was triggered by an external signal. A frame grabber (Dipix Corporation Model XPG-1000) was used to grab images from the camera for subsequent transfer to the computer for imaging processing.

A set of temperature-sensitive liquid crystal sheets was purchased from Edmund Scientific. According to the manufacturer, the sheets were produced by dispersing 3 to 5 μm cholesteric liquid crystals in a polymer matrix. For each sheet, the film was encapsulated between two sheets of Mylar for protection. One side of the sheet was coated with black ink. The set contains six sheets of liquid crystal, each sensitive to a different range of temperatures, namely, 20–25, 25–30, 30–35, 35–36, 35–40, and 40–45 °C.

RESULTS AND DISCUSSION

Temperature-sensitive cholesteric liquid crystal was selected for this study because it is known that changes in temperature lead to rapid changes in the absorption and refractive index of the liquid crystal.[19,20] Furthermore, liquid crystal films that are sensitive to different temperature ranges are commercially available.

Because the cholesteric liquid crystal absorbs NIR light through the overtone and combination absorption of the C–H, O–H, and N–H groups, irradiating it with an NIR laser will lead to a change in its temperature, which, in turn, produces changes in the absorption and refractive index. Such changes were, in fact, observed when the liquid crystal was irradiated with the NIR laser at 805 nm. Without knowing the structure of the liquid crystal, it is difficult to determine the exact transitions that are responsible for the absorption. It may be possible that the overtones and combination transitions of the C–H groups are responsible for the absorption.[15]

Since changes induced in the liquid crystal are in the visible region, they can be readily monitored with a visible silicon area camera. As this is an area camera, each image it records corresponds to a two-dimensional (2D) picture of the sample. It can, therefore, be used to record rapid changes in the liquid crystal either as a function of time (i.e., quickly record picture at a fixed wavelength as a function of time) or as a function of wavelength (i.e.,

rapidly record images at different wavelengths) but not both (i.e., simultaneously varying both time and wavelength). This limitation is due to the fact that changes in the absorption and refractive index of the liquid crystal with time are faster than the time required to change the wavelength setting of the AOTF and to record a new image. As a consequence, two sets of experiments were designed to demonstrate the operation of the image spectrometer and the properties of the liquid crystal: images were recorded as a function of time and as a function of wavelength.

In the first set of experiments, the liquid crystal was irradiated by a pulsed NIR diode laser, and changes in the absorption and the refractive index of the liquid crystal were monitored by rapidly and consecutively recording multiple images as a function of time at a single wavelength. Subsequently, the recording wavelength was changed and a new set of images were recorded. The procedure was repeated for several wavelengths so that subsequent treatment of images would enable the calculation of spectra that show the changes in the absorption and refractive index as a function of time (for many illuminating wavelengths).

In the second set of experiments, the liquid crystal was irradiated by the same NIR diode laser operating not in the pulse mode but rather in the continuous mode. Changes in the sample were monitored by illuminating it with a monochromatic light from the AOTF. The AOTF was scanned rapidly, and one image was recorded for each wavelength. Subsequent treatment of the recorded images (for many wavelengths) will enable the calculation of spectra that show changes in the absorption and refractive index as a function of wavelength. Changes in the sample with time were negligible in this case because the sample was irradiated with a continuous NIR laser. As a consequence, its photo-induced changes are presumably a steady state.

Multispectral Imaging as a Function of Time. The timing of the first set of experiments is shown in Fig. 2 and can be explained as follows: While under illumination with a monochromatic diffracted light from the AOTF, the sample was irradiated by a single pulse from the NIR diode laser. An external pulse was generated by a computer (trace #2 of Fig. 2), and the positive slope of the pulse started the diode laser. An external delay line, provided by the timing controller, was used to adjust the firing time of the diode laser (trace #4). The Dalsa charge-coupled device (CCD) camera was operated in the free running mode; i.e., it continuously recorded images (trace #1). The negative slope of the pulse generated by the computer started the frame grabber (trace #3). The frame grabber was operated in the multiple grabbing mode and was set to acquire a set of multiple and consecutive images as fast as it could grab them from the camera (for a set duration, which in this study was 1.5 s). These frames were then consecutively stored in the memory of the frame-grabber board. The maximum number of frames which the frame grabber can grab in a given time is defined by two factors: the total number of frames stored in the frame grabber and the speed necessary to transfer the frames. The maximum number of frames that can be stored is dependent on the memory of the frame-grabber board and size of frame. The maximum speed of

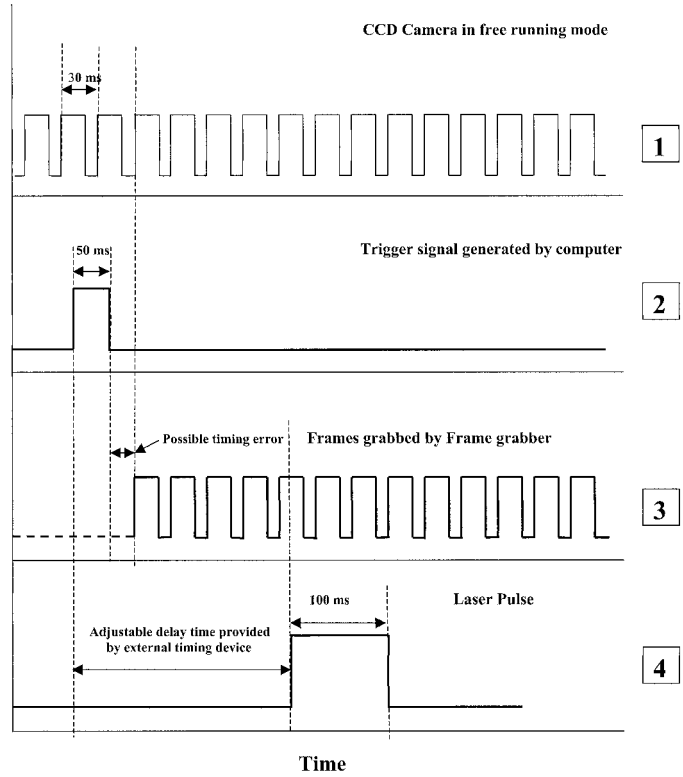

FIG. 2. Timing sequence of the multispectral imaging measurements.

frame transfer is defined by the specifications and the exposure time (i.e., the integration time) of the camera. This rate cannot, however, exceed the maximum clock frequency that supports the Digital Camera Module component of the Dipix XPG-1000 frame grabber, which in this case is 50 MHz at 8 bits/pixel. In this study, with the Dalsa CA-D8 camera and the 16 Mbyte memory on the XPG-1000 board, the maximum number of frames that the grabber can grab is 33 frames/s. Therefore, a total of 50 images can be grabbed by the grabber in the 1.5 s duration used in this study.

As described above, by the use of the signal generated by the computer and the delay line provided by the timing controller, the firing of the diode laser pulse can be precisely controlled. However, because the CCD camera was operated not in the snap-scan mode but rather in the free-running mode (i.e., images are continuously recorded), and the frame grabber was started by the negative slope of the same signal generated by the computer, it was difficult to precisely control the start of the frame grabbing (i.e., the grabber can only grab an entire frame from its beginning). As a consequence, there may by some error due to this timing mismatch (trace #3). However, the error produced by this mismatch is not more than one frame, i.e, ± 15 ms.

With the delay line shown in Fig. 2, four images of the sample were recorded and grabbed prior to the laser pulse. However, the number of images that are recorded before the laser pulse is not fixed at four frames as in this study. It can be adjusted by the use of an appropriate delay line. As a consequence, events occurring in the sample can be monitored at any time (i.e., before, during, and after the laser pulse) for any duration of time. This timing arrangement made it possible to precisely deter-

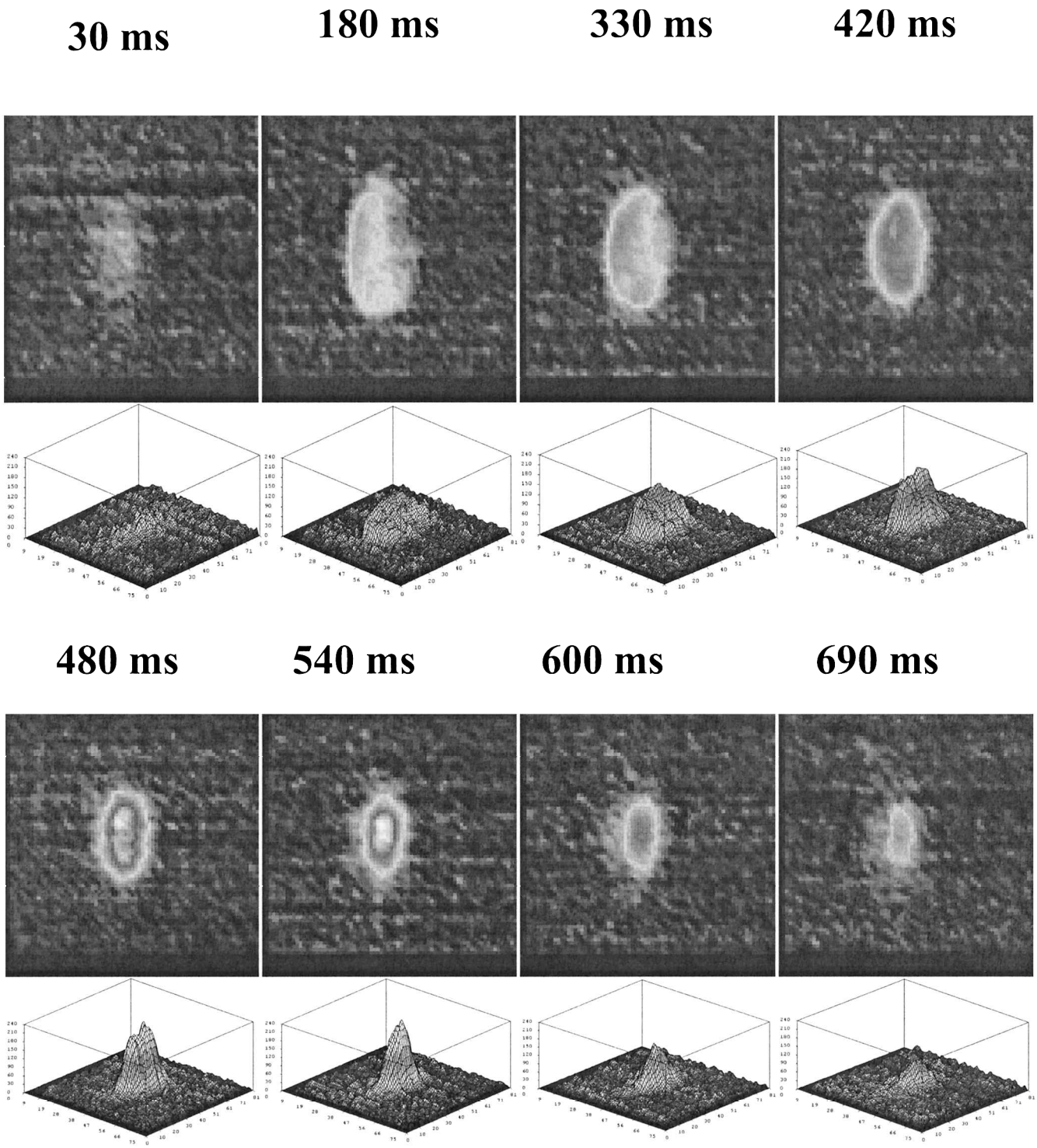

FIG. 3. 2D (upper) and 3D (lower) plots of images of reflected light intensity at 600 nm taken for the 30–35 °C liquid crystal at different times after the start of the 805 nm diode laser pulse.

mine the timing of the experiment in the recorded images, namely, the time $t = 0$ when the laser pulse was first incident to the sample. It also offers background images which can be used for background correction. The duration of the laser pulse used in this study was 100 ms. As shown in Fig. 2, there were, therefore, about three images of the sample during the time it was irradiated by the laser pulse. Image number 8 and thereafter are those of the sample after the pulse laser went off. From the same area, which in this case corresponds to a square of 7×7 pixels, the intensity of light was calculated from each of the images beginning with image number 8. This approach allows the construction of spectra that show the changes of the liquid crystal induced by the NIR pulse laser.

Two- and three-dimensional (3D) plots of some of images of the reflected light intensity at 600 nm, taken at different times (30, 180, 330, 420, 480, 540, 600, and

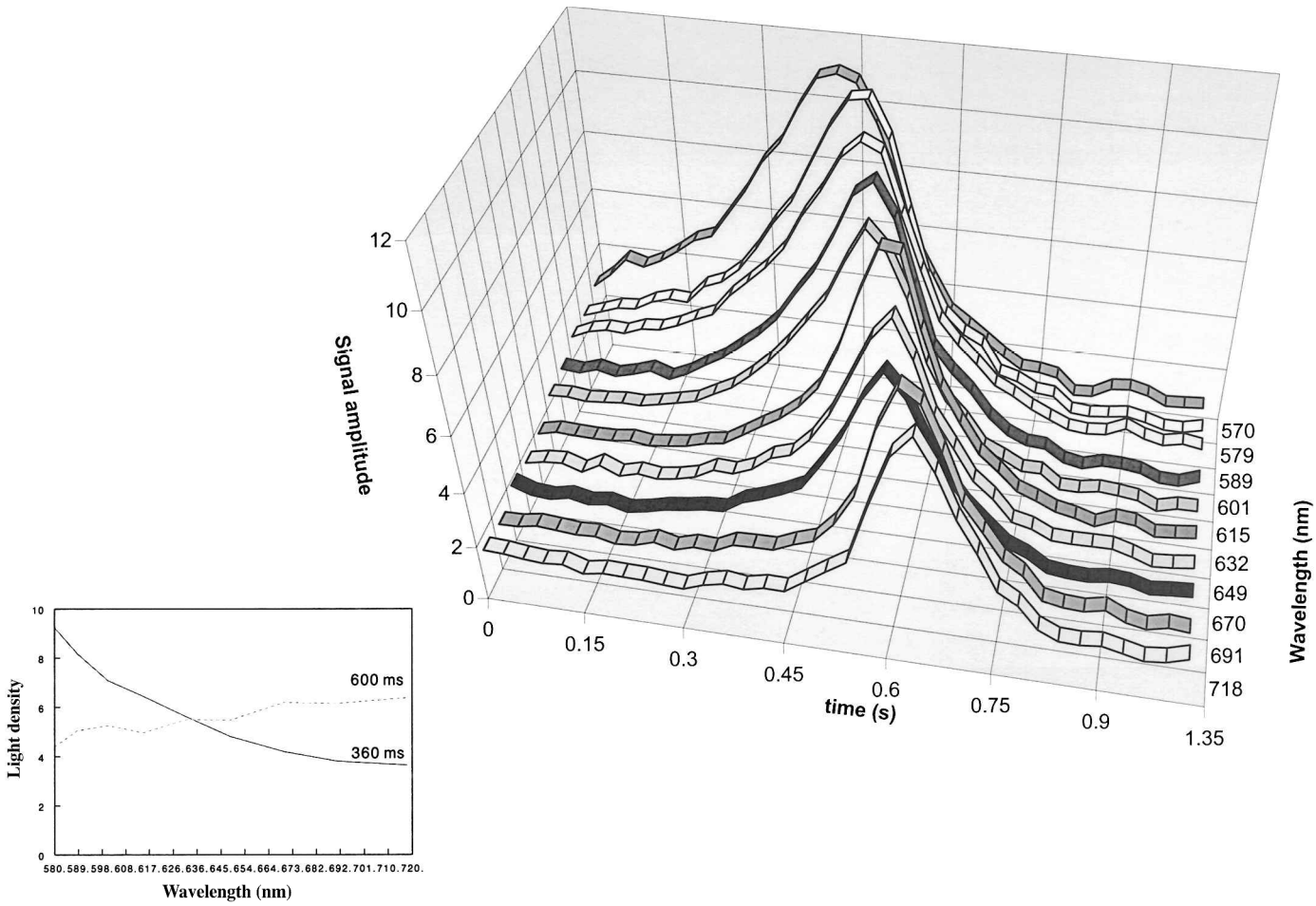

FIG. 4. Changes in the reflected light intensity at different wavelengths, plotted as a function of time for 30–35 °C liquid crystal.

690 ms after the start of the laser pulse) for the liquid crystal that is sensitive in the 30–35 °C temperature range are shown in Fig. 3. As illustrated, the changes in the reflected light intensity increased concomitantly with time until about 540 ms when it went through a maximum value; thereafter it decreased. The results can be better visualized in Fig. 4, which shows the changes in the intensity of light reflected from the liquid crystal at different illumination wavelengths plotted as a function of time. These spectra were calculated by comparing data for each square of 7 × 7 pixels from each image. As illustrated, heating by an NIR pulse led to changes in the liquid crystal. About 360 ms after the NIR laser pulse, the liquid crystal underwent changes in the visible region at around 570 nm. The changes shifted toward longer wavelength concomitantly with time, i.e., maximum changes at about 600 ms shifted to 718 nm. Interestingly, initial changes in the shorter wavelength region at the beginning were relatively slower than those at the longer wavelengths at the latter time; i.e., the slopes of the bands were relatively smaller for bands at shorter wavelengths than those for bands at longer wavelengths. A better illustration of the effect can be seen in the insert of Fig. 4 which was constructed from the data in Fig. 4 to show the responses of the liquid crystal 360 and 600 ms after the laser pulse, plotted as a function of wavelength. As illustrated, 360 ms after the laser pulse, the changes in the liquid crystal decreased rapidly as a function of time. Conversely, the signal plotted 600 ms after the laser pulse shows the increase in the intensity of the reflected light as a function of wavelength. However, the slope of the build-up at the longer time scale was smaller than that of the decay of the shorter time.

It is important to point out that changes in the temperature are known to produce changes in the absorption and refractive index of liquid crystals. Because in this experiment the intensity of the light diffuse-reflected from the sample was measured, it is not possible to separate the change in the absorption from that of the refractive index. The two effects (change in absorption and change in the refractive index) produce a visible change in the liquid crystal, and this was observed by the recorded images.

Measurements were also performed on two other liquid crystals that are specified to be sensitive in the temperature ranges of 35–40 and 40–45 °C. Results are shown in Figs. 5 and 6, respectively. Similar to the 30–35 °C liquid crystal, these two liquid crystals also exhibit changes in the intensity of reflected light as a function of wavelength; namely, the changes at shorter wavelength are relatively slower and occur at an earlier time than those at the longer wavelength. Interestingly, the magnitude of the changes in the higher temperature liquid crystal (i.e., 40–45 °C) is smaller but occurs much faster

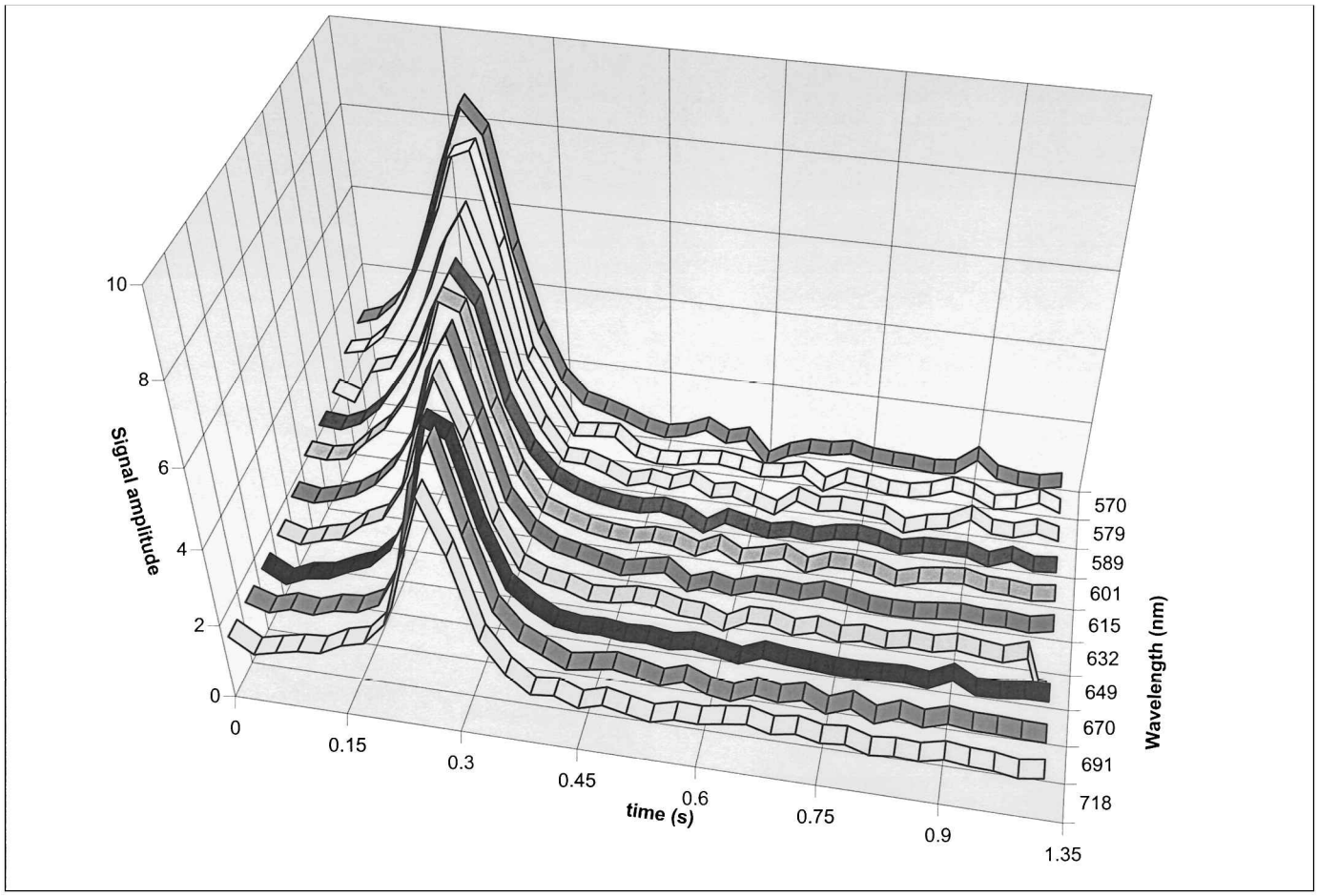

FIG. 5. Changes in the reflected light intensity at different wavelengths, plotted as a function of time for 35–40 °C liquid crystal.

than those for lower temperature samples (30–35 °C). For the same wavelength range, the intensity of the reflected light for the 40–45 °C liquid crystal is lower and was completed at 150 ms after the laser pulse, whereas it took at least 800 ms for the more intense reflected beam from the 30–35 °C sample to completely change. The 35–40 °C sample falls between these two samples; i.e., its changes were completed 450 ms after the laser pulse.

Multispectral Imaging as a Function of Wavelength. The second set of experiments was designed to demonstrate the ability of this imaging spectrometer for the rapid recording of images at different wavelengths. This was accomplished by irradiating the liquid crystal with the NIR diode laser operating in the continuous mode and rapidly scanning the AOTF to change the wavelength of the illuminating light. As described in the previous paragraph, by irradiation of the liquid crystal with a continuous NIR light, its photo-induced changes reach a steady state, thereby eliminating complications associated with the changes in the sample with time. The frame-grabbing mode in this case was slightly different from that used in the previous set of experiments. The grabber still tries to grab as many images as quickly as it can. However, the rapid scanning of the AOTF imposes an additional requirement. As a consequence of this requirement, the AOTF was set at one wavelength (by the computer) for the camera to record one image. The frame grabber rapidly grabs the recorded image and then rapidly copies it into the next available buffer in its memory for storing. The time spent during this frame transfer enabled the AOTF to be changed to the next wavelength. Again an image at this wavelength was grabbed and transferred to the grabber's memory for storage. The process continues (i.e., one frame per one wavelength) until the frame grabber memory was full of frames. At that time, all of the stored frames were transferred to the computer. Because of the extra time required in this mode of operation (i.e., to transfer frames and to scan the AOTF), the total number of frames that can be grabbed was only 16 frames/s, which is relatively lower than the 33 frames/s achieved in the previous experiments in which the AOTF was set at a constant wavelength during the frame grabbing.

Spectra that illustrate changes in the intensity of the reflected light plotted as a function of wavelength for the 30–35 °C liquid crystal are shown in Fig. 7. These spectra were taken when the liquid crystal was irradiated with the continuous-wave NIR diode laser with different laser powers (from 27 to 65 mW), and the AOTF was scanned from 460 to 580 nm at 2 nm intervals. A total of 60 images was needed to construct one spectrum. As described in the previous paragraph, in this configuration the instrument can grab 16 frames/s. As a consequence, it required 3.8 s to acquire 60 images from which one spectrum was calculated.

Spectra of the sample at different laser powers were

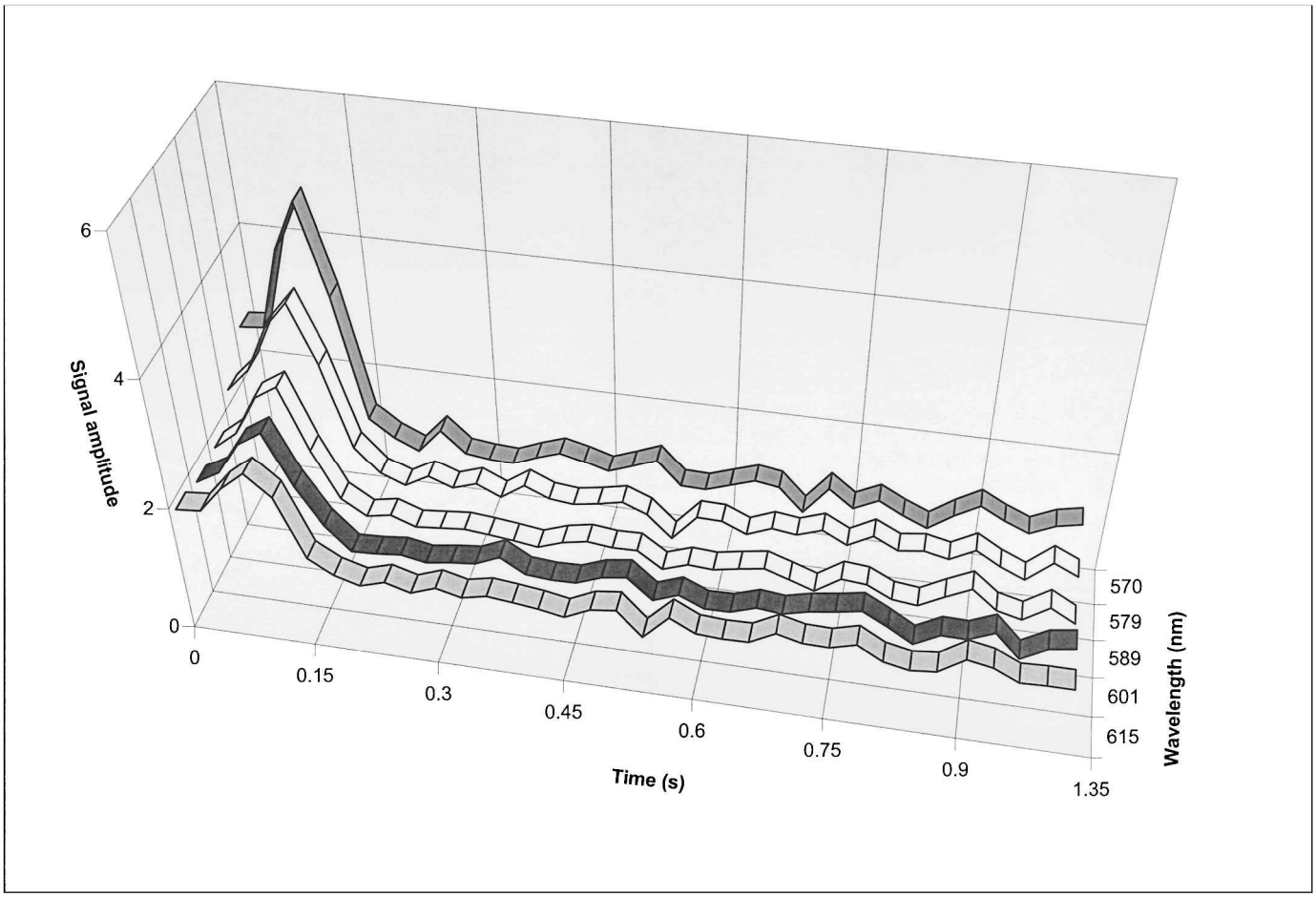

FIG. 6. Changes in the reflected light intensity at different wavelengths, plotted as a function of time for 40–45 °C liquid crystal.

calculated from recorded images. The calculated spectra were then corrected for the differences in the intensity of the illuminating halogen tungsten lamps, and the resulting spectra are shown in Fig. 7. The correction was necessary because it is known that the spectral output of the halogen tungsten lamp is dependent on wavelength. The correction was accomplished by replacing the sample with a mirror to record the spectral output of the halogen tungsten lamp for the subsequent correction (by dividing the sample spectrum by the corresponding lamp spectral out-

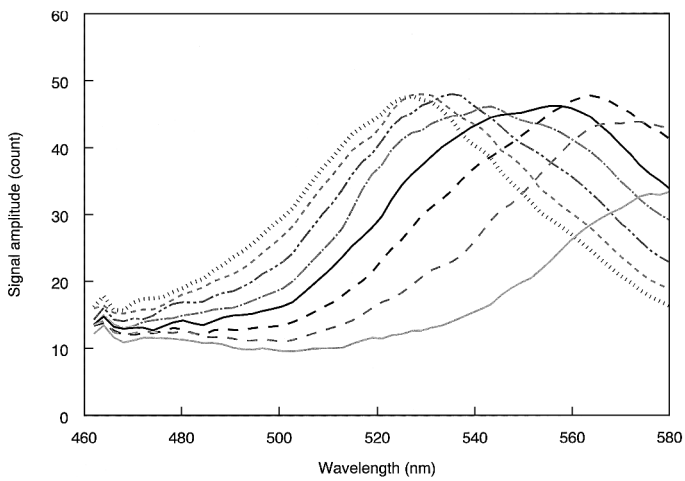

FIG. 7. Changes in the reflected light intensity as a function of wavelength for the 30–35 °C liquid crystal irradiated with a continuous-wave diode laser with different powers: (———) 34 mW; (- - - - - -) 36 mW; (– – –) 39 mW; (———) 41 mW; (— - — - —) 43 mW; (— - — — - — —) 45 mW; (- - - - - - - - - - - - -) 48 mW; and (·····) 50 mW.

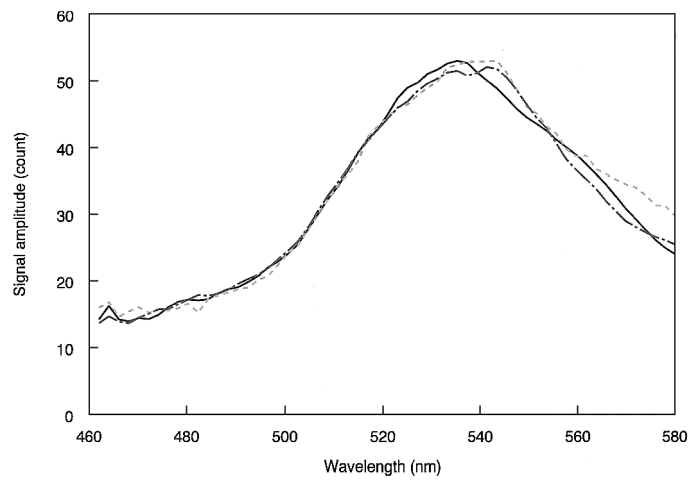

FIG. 8. Changes in the reflected light intensity as a function of wavelength for the 30–35 °C liquid crystal (———); the 35–40 °C liquid crystal (- - - - - - - - -); and the 40–45 °C liquid crystal (—··—··) irradiated with a continuous-wave diode laser with 45, 56, and 63 mW power, respectively.

put). It is important to point out that the assumption that the sample was at steady state is valid because the same spectra were obtained (for the same NIR laser power).

As illustrated in Fig. 7, increasing the power of the NIR irradiating laser light shifted the spectra toward shorter wavelengths: the peak at 565 nm, which was obtained with a 39 mW laser power, shifted to 556 nm when the laser power was increased to 41 mW, to 550 nm for 43 mW, to 538 nm for 45 mW, and to 530 nm for 48 and 50 mW. This pattern may be due to the fact that increasing the power of the irradiating laser provides a higher temperature change in the sample, which, as a consequence, shifts the changes toward shorter wavelength (higher energy) region.

A similar effect can also be seen in Fig. 8, which plots the changes for three different liquid crystal sheets (30–35, 35–40, and 40–45 °C) as a function of wavelength. Different laser powers were used to measure these spectra: 45 mW for the 30–35 °C sample, 56 mW for the 35–40 °C sample, and 63 mW for the 40–45 °C sample. As illustrated, it was necessary to increase the diode laser power by 24 and 40% (from 45 to 56 and 63 mW) in order to produce change for the 35–40 and 40–45 °C samples, respectively, at the same wavelength as the 30–35 °C sample. This requirement was as expected, because higher laser power is needed to generate sufficient temperature change to ensure that it can produce changes in liquid crystals that are sensitive to relatively higher temperatures (35–40 and 40–45 °C).

In summary, it has been demonstrated that a new multispectral imaging spectrometer with millisecond resolution can be developed by use of an AOTF for spectral tuning and a simple progressive scan camera capable of snapshot operation for recording. The fast multispectral imaging can be performed in two configurations: recording 2D images as a function of time or as a function of wavelength. In the first configuration, as many images as possible are recorded, grabbed, and stored per one wavelength. Upon completion, the AOTF is scanned to a new recording wavelength and a new set of images are recorded. It was found that in this configuration, the imaging spectrometer is capable of recording, grabbing, and storing up to 33 images per s (i.e., 30 ms per image). Because the recording camera is synchronized with an external signal and a delay time can be installed to appropriately adjust the duration between the start of an event and the recording and grabbing of the image, the time resolution of the spectrometer is not limited to 30 ms but rather can be adjusted to a shorter or longer time scale. In the second configuration, the recording wavelength is rapidly scanned (by means of the AOTF), and only one image is rapidly recorded, grabbed, and stored for each wavelength. Because additional time is needed to scan the AOTF, the maximum number of images that can be grabbed in this case is 16 frames per second. The operation of the imaging spectrometer was demonstrated in the investigation, which aims to study the spectral, temporal, and spatial response of a variety of cholesteric liquid crystals sensitive to different temperature ranges.

Preliminary applications of the imaging spectrometer include measurements of photo-induced changes in temperature-sensitive cholesteric liquid crystals as a function of time and wavelength. It was found that irradiating with a pulsed NIR diode laser of 805 nm led to changes in the liquid crystal. The changes were found to be varied with time and wavelength; namely, about 360 ms after the NIR laser pulse the liquid crystal underwent changes in the visible region around 570 nm. The changes shifted toward longer wavelength concomitantly with time; i.e., maximum change at about 600 ms shifted to 718 nm. Under steady-state conditions, i.e., when they were irradiated with a continuous-wave NIR diode laser, the liquid crystals underwent changes that varied with the laser power. Specifically, for the 30–35 °C liquid crystal, the maximum change at 570 nm obtained with 38 mW power shifted to 560 nm when the power was increased to 41 mW. Higher laser power was needed to produce changes in higher temperature liquid crystal at the same wavelength as those for lower temperature samples.

The present study of liquid crystals is an example that illustrates the type of measurements that can be performed by using this time-resolved multispectral imaging spectrometer. It should be noted that the ability to perform multispectral imaging in the millisecond time scale is important not only for investigations of rapid photochemical and photophysical processes but also for low S/N measurements as well as for measurements where the samples are chemically stable but not in the same position. Measuring in a millisecond time scale enables this imaging instrument to rapidly acquire multiple images of samples with low S/N for subsequent signal averaging or increasing the integration time of measurements. The instrument is also particularly suited for measurements where the sample and/or the instrument are on the move, i.e, for remote sensing and online quality control and assurance. Furthermore, the wavelength region is not limited to the visible as in this study but can be extended to the near- and middle-IR. In fact, with the Dalsa CCD camera replaced by the InGaAs NIR camera that was used in our earlier studies,[5–7] NIR multispectral imaging in the millisecond time scale can be readily accomplished. These possibilities are the subject of intense investigation.

ACKNOWLEDGMENTS

Acknowledgment is made to the National Institutes of Health, National Center for Research Resources, Biomedical Technology Program for financial support of this research.

1. M. D. Morris, *Microscopic and Spectroscopic Imaging of the Chemical State* (Marcel Dekker, New York, 1993).
2. C. D. Tran, Anal. Chem. **64,** 971A (1992).
3. C. D. Tran, Talanta, **45,** 237 (1997).
4. H. R. Morris, C. C. Hoyt, and P. J. Treado, Appl. Spectrosc. **48,** 857 (1994).
5. E. N. Lewis, P. J. Treado, R. C. Reeder, G. M. Story, A. E. Dowrey, C. Marcott, and I. W. Levin, Anal. Chem. **67,** 3377 (1995).
6. E. N. Lewis, A. M. Gorbach, C. Marcott, and I. W. Levin, Appl. Spectrosc. **50,** 263 (1996).
7. C. D. Tran, Y. Cui, and S. Smirnov, Anal. Chem. **70,** 4701 (1998).
8. M. Fischer and C. D. Tran, Anal. Chem. **71,** 953 (1999).
9. M. Fischer and C. D. Tran, Anal. Chem. **71,** 2255 (1999).
10. P. J. Treado, I. W. Levin, and E. N. Lewis, Appl. Spectrosc. **46,** 553 (1992).
11. P. J. Treado, I. W. Levin, and E. N. Lewis, Appl. Spectrosc. **48,** 607 (1994).
12. E. N. Lewis, L. H. Kidder, J. F. Arens, M. C. Peck, and I. W. Levin, Appl. Spectrosc. **51,** 563 (1997).

13. P. Colarusso, L. H. Kidder, I. W. Levin, J. C. Fraser, J. F. Arens, and E. N. Lewis, Appl. Spectrosc. **52,** 106A (1998).
14. C. M. Snively and J. L. Koenig, Macromolecules **31,** 3753 (1998).
15. B. L. McClain, J. Ma, and D. Ben-Amotz, Appl. Spectrosc. **53,** 1118 (1999).
16. K. A. Christensen and M. D. Morris, Appl. Spectrosc. **52,** 1145 (1998).
17. M. S. Baptista, C. D. Tran, and G. Gao, Anal. Chem. **68,** 971 (1996).
18. M. J. Politi, C. D. Tran, and G. Gao, J. Phys. Chem. **99,** 14137 (1995).
19. S. D. Jacobs, *Liquid Crystals for Optics* (SPIE Publishing, Bellingham, Washington, 1992).
20. P. S. Drzaic, *Liquid Crystal Dispersions* (World Scientific Publishing, River Edge, New Jersey 1995).